Computational Study of C−C Activation of 1,3-Dimesitylimidazol-2-ylidene (IMes) at Ruthenium: The Role of Ligand Bulk in Accessing Reactive Intermediates

Richard A. Diggle,[†] Stuart A. Macgregor,*[,†] and Michael K. Whittlesey*[,‡]

School of Engineering and Physical Sciences, William Perkin Building, Heriot-Watt University, Edinburgh, EH14 4AS, U.K., and Department of Chemistry, University of Bath, Claverton Down, Bath, BA2 7AY, U.K.

Received October 1, 2007

Density functional theory calculations have been employed to model phosphine substitution in $Ru(PPh_3)_3(CO)(H)_2$ to form $Ru(IMes)(PPh_3)_2(CO)(H)_2$ ($\mathbf{1}_{mono}$) and $Ru(IMes)_2(PPh_3)(CO)(H)_2$ ($\mathbf{1}_{bis}$), as well as the novel C(aryl)−C(sp^3) intramolecular bond activation of the IMes ligand in $\mathbf{1}_{bis}$. The computed ligand exchange energies show that $\mathbf{1}_{bis}$ is unstable with respect to displacement of IMes by PPh_3 and will thus re-form $\mathbf{1}_{mono}$ over time. PPh_3/IMes substitution also leads to a significant labilization of the PPh_3 ligand *trans* to hydride, a result of increasing steric encumbrance upon the introduction of the bulky IMes ligands. The energetics of intramolecular C−C and C−H activation have been computed for both 16e $Ru(IMes)_n(PPh_3)_{3-n}(CO)$ and 14e $Ru(IMes)_n(PPh_3)_{2-n}(CO)$ species ($n = 1$ or 2) and indicate that the introduction of a second IMes ligand does not significantly promote the actual C−C activation step. Instead the need to have two IMes ligands present in the metal coordination sphere before C−C activation can occur is linked to the promotion of PPh_3 loss in $\mathbf{1}_{bis}$, which makes the formation of unsaturated species such as $Ru(IMes)_2(CO)$ particularly accessible.

Introduction

Over the last 15 years N-heterocyclic carbenes (NHCs) have become extremely popular as ligands in transition metal (TM) chemistry.[1] As with phosphines, variation in the steric and electronic properties of the NHC promises control of the metal coordination environment; indeed early reports did refer to NHCs as phosphine mimics.[2] NHCs have additional properties as ligands that are thought to be particularly beneficial to catalysis. NHCs form strong bonds to TM centers,[3] a feature attributed to powerful σ-donation from the carbene carbon lone pair[4] (although the potential of NHCs to act as weak π-acceptors or even π-donors has also been discussed[5]). Moreover, it was also thought that NHCs would be less prone to ligand-based decomposition reactions than phosphines.[6b] These factors have led to an explosion of interest in the use of NHCs as auxiliary ligands in catalysis,[6,7] and one particularly notable success was the development of Grubbs' second-generation alkene metathesis catalysts, where replacement of PCy_3 with 1,3-dimesitylimidazol-2-ylidene (IMes) led to significant improvements in catalytic activity.[8,9]

More recently, however, the view of NHCs as strongly bound inert spectator ligands has had to be modified due to the emergence of a range of NHC-based reactions.[10] In some cases TM−NHC bonds have been found to be unexpectedly labile, and dissociation leads to a loss of control of the metal

* Corresponding author. E-mail: s.a.macgregor@hw.ac.uk.
† Heriot-Watt University.
‡ University of Bath.

(1) (a) Herrmann, W. A.; Köcher, C. *Angew. Chem., Int. Ed.* **1997**, *36*, 2162. (b) Bourissou, D.; Guerret, O.; Gabbaï, F. P.; Bertrand, G. *Chem. Rev.* **2000**, *100*, 39. (c) Weskamp, T.; Böhm, V. P. W.; Herrmann, W. A. *J. Organomet. Chem.* **2000**, *600*, 12. (d) Scott, N. M.; Nolan, S. P. *Eur. J. Inorg. Chem.* **2005**, 1815. (e) Hahn, F. E. *Angew. Chem., Int. Ed.* **2006**, *45*, 1348.

(2) Öfele, K.; Herrmann, W. A.; Mihalios, D.; Elison, M.; Herdtweck, E.; Scherer, W.; Mink, J. *J. Organomet. Chem.* **1993**, *459*, 177.

(3) (a) Huang, J.; Schanz, H.-J.; Stevens, E. D.; Nolan, S. P. *Organometallics* **1999**, *18*, 2370. (b) Huang, J.; Jafarpour, L.; Hillier, A. C.; Stevens, E. D.; Nolan, S. P. *Organometallics* **2001**, *20*, 2878. (c) Hillier, A. C.; Sommer, W. J.; Yong, B. S.; Petersen, J. L.; Cavallo, L.; Nolan, S. P. *Organometallics* **2003**, *22*, 4322. (d) Dorta, R.; Stevens, E. D.; Scott, N. M.; Costabile, C.; Cavallo, L.; Hoff, C. D.; Nolan, S. P. *J. Am. Chem. Soc.* **2005**, *127*, 2485.

(4) (a) Green, J. C.; Scurr, R. G.; Arnold, P. L.; Cloke, F. G. N. *Chem. Commun.* **1997**, 1963. (b) Tafipolsky, M.; Scherer, W.; Öfele, K.; Artus, G.; Pedersen, B.; Herrmann, W. A.; McGrady, G. S. *J. Am. Chem. Soc.* **2002**, *124*, 5865. (c) Cavallo, L.; Correa, A.; Costabile, C.; Jacobsen, H. *J. Organomet. Chem.* **2005**, *690*, 5407. (d) Díez-González, S.; Nolan, S. P. *Coord. Chem. Rev.* **2007**, *251*, 874.

(5) (a) Hu, X.; Tang, Y.; Gantzel, P.; Meyer, K. *Organometallics* **2003**, *22*, 612. (b) Hu, X.; Castro-Rodriguez, I.; Olsen, K.; Meyer, K. *Organometallics* **2004**, *23*, 755. (c) Scott, N. M.; Dorta, R.; Stevens, E. D.; Correa, A.; Cavallo, L.; Nolan, S. P. *J. Am. Chem. Soc.* **2005**, *127*, 3516. (d) Jacobsen, H.; Correa, A.; Costabile, C.; Cavallo, L. *J. Organomet. Chem.* **2006**, *691*, 4350.

(6) (a) Nolan, S. P. *N-Heterocyclic Carbenes in Synthesis*; Wiley-VCH: Weinheim, 2006. (b) *N-Heterocyclic Carbenes in Transition Metal Catalysis*; Glorius, F. A., Ed.; Springer: Berlin, 2007.

(7) (a) Herrmann, W. A.; Weskamp, T.; Böhm, V. P. W. *Adv. Organomet. Chem.* **2002**, *48*, 1. (b) Herrmann, W. A. *Angew. Chem., Int. Ed. Engl.* **2002**, *41*, 1290. (c) Peris, E.; Crabtree, R. H. *Coord. Chem. Rev.* **2004**, *248*, 2239. (d) César, V.; Bellemin-Laponnaz, S.; Gade, L. *Chem. Soc. Rev.* **2004**, *9*, 619. (e) Sommer, W. J.; Weck, M. *Coord. Chem. Rev.* **2007**, *251*, 860. (f) Dragutan, V.; Dragutan, I.; Delaude, L.; Demonceau, A. *Coord. Chem. Rev.* **2007**, *251*, 765. (g) Kantchev, E. A. B.; O'Brien, C. J.; Organ, M. G. *Angew. Chem. Int. Ed.* **2007**, *46*, 2768.

(8) (a) Weskamp, T.; Schattenmann, W. C.; Spiegler, M.; Herrmann, W. A. *Angew. Chem., Int. Ed.* **1998**, *37*, 2490. (b) Scholl, M.; Trnka, T. M.; Morgan, J. P.; Grubbs, R. H. *Tetrahedron Lett.* **1999**, *40*, 2247. (c) Scholl, M.; Ding, S.; Lee, C. W.; Grubbs, R. H. *Org. Lett.* **1999**, *1*, 953. (d) Huang, J.; Stevens, E. D.; Nolan, S. P.; Petersen, J. L. *J. Am. Chem. Soc.* **1999**, *121*, 2674. (e) Jafarpour, L.; Nolan, S. P. *Adv. Organomet. Chem.* **2001**, *46*, 181.

(9) (a) For an overview of this area, see: Fürstner, A. *Angew. Chem., Int. Ed.* **2000**, *39*, 3012. (b) Trnka, T. M.; Grubbs, R. H. *Acc. Chem. Res.* **2001**, *34*, 18. (c) Jafarpour, L.; Nolan, S. P. *J. Organomet. Chem.* **2001**, *617–618*, 17. (d) Grubbs, R. H. *Tetrahedron* **2004**, *60*, 7117. (e) Deshmukh, P. H.; Blechert, S. *Dalton Trans.* **2007**, 2479.

(10) For a review of these processes, see: Crudden, C. M.; Allen, D. P. *Coord. Chem. Rev.* **2004**, *248*, 2247.

10.1021/om700977f CCC: $40.75
Publication on Web 01/23/2008

coordination geometry.[11] NHC ligands can also be lost via reductive elimination of imidazolium salts.[12] Alternatively, the NHC ligand may stay bound to the metal center but is modified by some intramolecular reaction. Examples include migratory insertion[13,14] or even cleavage of the N−C(substituent) bond.[15] One of the most common types of such NHC-based reactivity involves cyclometalation, and many cases involving C−H activation of both N-alkyl[5c,16]and N-aryl[11f,16g,17] substituents have now been documented.[18]

One particularly well-defined example of an NHC cyclometalation reaction has been reported for Ru(IMes)(PPh_3)$_2$(CO)(H)$_2$ (**1**$_{mono}$).[19] Reaction of **1**$_{mono}$ with alkenes at room temperature results in intramolecular C−H activation to give **3**$_{mono}$ (eq 1). In this process the alkene acts as a hydrogen acceptor and forms a Ru(0) intermediate such as Ru(IMes)(PPh_3)$_2$(CO), **2**$_{mono}$, where C−H activation can then take place. **1**$_{mono}$ can be re-formed from **3**$_{mono}$ upon addition of H_2, and this feature has proved particularly useful in catalytic transfer hydrogenation reactions involving alcohols.[20]

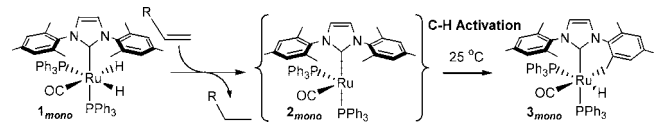

(1)

More unusually, this system can also be induced to undergo an alternative intramolecular bond activation reaction involving a much rarer C−C bond cleavage (eq 2). Heating **1**$_{mono}$ to 80 °C with excess IMes results in the formation of PPh_3/IMes-substituted **1**$_{bis}$, which upon further heating undergoes C(sp^2)−C(sp^3) bond cleavage to produce **5**. The details of the transformation of **1**$_{bis}$ to **5**, which also features loss of CH_4 and IMes/PPh_3 substitution, are not clear; however, formation of the bis-IMes complex is central to the C−C activation, as no reaction is seen upon heating **1**$_{mono}$ alone. Unlike the C−H activation linking **1**$_{mono}$ and **3**$_{mono}$, the formation of **5** is irreversible and so results in a permanently modified NHC ligand.

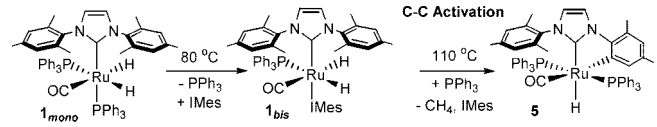

(2)

The observation of C−C activation in **1**$_{bis}$ is important, not only because of the ramifications for the stability of TM−NHC complexes but also because such C−C bond cleavage is an inherently difficult process. We have therefore undertaken a series of computational studies to define the factors that promote this unusual reaction. Initially we had thought that the ability of **1**$_{bis}$ to perform C−C activation was due to the presence of two strongly donating NHC ligands. Any unsaturated intermediates derived from this species would then be highly electron-rich and so may be capable of cleaving a normally unreactive C(sp^2)−C(sp^3) bond. In fact, calculations on intermolecular bond activation processes at model 16e intermediates of the type Ru(IH)$_n$(PH_3)$_{3-n}$(CO) (IH = imidazol-2-ylidene; n = 0, 1, 2) showed this assertion to be incorrect, as PH_3/IH substitution caused no significant changes in the energetics of oxidative addition in these systems.[21] Therefore we have extended our work to consider the effect of PPh_3/IMes substitution in the full experimental systems **1**$_{mono}$ and **1**$_{bis}$. As well as considering bond activation at unsaturated intermediates derived from these species we have also computed the energetics of PPh_3/IMes substitution in these systems as well as the parent tris-PPh_3 species, Ru(PPh_3)$_3$(CO)(H)$_2$ (**6**). The results provide a further

(11) (a) Hitchcock, P. B.; Lappert, M. F.; Pye, P. L. *J. Chem. Soc., Dalton Trans.* **1978**, 826. (b) Doyle, M. J.; Lappert, M. F.; Pye, P. L.; Terreros, P. *J. Chem. Soc., Dalton Trans.* **1984**, 2355. (c) Titcomb, L. R.; Caddick, S.; Cloke, F. G. N.; Wilson, D. J.; McKerrecher, D. *Chem. Commun.* **2001**, 1388. (d) Simms, R. W.; Drewitt, M. J.; Baird, M. C. *Organometallics* **2002**, *21*, 2958. (e) Lewis, A. K. de K.; Caddick, S.; Cloke, F. G. N.; Billingham, N. C.; Hitchcock, P. B.; Leonard, J. *J. Am. Chem. Soc.* **2003**, *125*, 10066. (f) Trnka, T. M.; Morgan, J. P.; Sanford, M. S.; Wilhelm, T. E.; Scholl, M.; Choi, T. L.; Ding, S.; Day, M. W.; Grubbs, R. H. *J. Am. Chem. Soc.* **2003**, *125*, 2546. (g) Allen, D. P.; Crudden, C. M.; Calhoun, L. A.; Wang, R. Y. *J. Organomet. Chem.* **2004**, *689*, 3203.

(12) (a) McGuinness, D. S.; Cavell, K. J.; Skelton, B. W.; White, A. H. *Organometallics* **1999**, *18*, 1596. (b) McGuinness, D. S.; Cavell, K. J. *Organometallics* **2000**, *19*, 4918. (c) McGuinness, D. S.; Saendig, N.; Yates, B. F.; Cavell, K. J. *J. Am. Chem. Soc.* **2001**, *123*, 4029. (d) Nielsen, D. J.; Magill, A. M.; Yates, B. F.; Cavell, K. J.; Skelton, B. W.; White, A. H. *Chem. Commun.* **2002**, 2500. (e) Clement, N. D.; Cavell, K. J. *Angew. Chem., Int. Ed.* **2004**, *43*, 3845. (f) Cavell, K. J.; McGuinness, D. S. *Coord. Chem. Rev.* **2004**, *248*, 671. (g) Bacciu, D.; Cavell, K. J.; Fallis, I. A.; Ooi, L. *Angew. Chem., Int. Ed.* **2005**, *44*, 5282. (h) Graham, D. C.; Cavell, K. J.; Yates, B. F. *Dalton Trans.* **2005**, 1093. (i) Graham, D. C.; Cavell, K. J.; Yates, B. F. *Dalton Trans.* **2006**, 1768.

(13) (a) Danopoulos, A. A.; Tsoureas, N.; Green, J. C.; Hursthouse, M. B. *Chem. Commun.* **2003**, 756. (b) Hu, X. L.; Meyer, K. *J. Am. Chem. Soc.* **2004**, *126*, 16322. (c) Becker, E.; Stingl, V.; Dazinger, G.; Puchberger, M.; Mereiter, K.; Kirchner, K. *J. Am. Chem. Soc.* **2006**, *128*, 6572. (d) Becker, E.; Stingl, V.; Dazinger, G.; Mereiter, K.; Kirchner, K. *Organometallics* **2007**, *26*, 1531. (e) Fantasia, S.; Jacobsen, H.; Cavallo, L.; Nolan, S. P. *Organometallics* **2007**, *26*, 3286.

(14) For an instance where a CO ligand inserts into a mesityl substituent of IMes, see: Galan, B. R.; Gembicky, M.; Dominiak, P. M.; Keister, J. B.; Diver, S. T. *J. Am. Chem. Soc.* **2005**, *127*, 15702.

(15) (a) Caddick, S.; Cloke, F. G. N.; Hitchcock, P. B.; Lewis, A. K. de K. *Angew. Chem., Int. Ed.* **2004**, *43*, 5824. (b) Burling, S.; Mahon, M. F.; Powell, R. E.; Whittlesey, M. K.; Williams, J. M. J. *J. Am. Chem. Soc.* **2006**, *128*, 13702.

(16) (a) Prinz, M.; Grosche, M.; Herdtweck, E.; Herrmann, W. A. *Organometallics* **2000**, *19*, 1692. (b) Burling, S.; Mahon, M. F.; Paine, B. M.; Whittlesey, M. K.; Williams, J. M. J. *Organometallics* **2004**, *23*, 4537. (c) Dorta, R.; Stevens, E. D.; Nolan, S. P. *J. Am. Chem. Soc.* **2004**, *126*, 5054. (d) Cabeza, J. A.; del Río, I.; Miguel, D.; Sánchez-Vega, M. G. *Chem. Commun.* **2005**, 3956. (e) Scott, N. M.; Pons, V.; Stevens, E. D.; Heinekey, D. M.; Nolan, S. P. *Angew. Chem., Int. Ed.* **2005**, *44*, 2512. (f) Corberán, R.; Sanaú, M.; Peris, E. *Organometallics* **2006**, *25*, 4002. (g) Hanasaka, F.; Tanabe, Y.; Fujita, K.; Yamaguchi, R. *Organometallics* **2006**, *25*, 826. (h) Spencer, L. P.; Beddie, C.; Hall, M. B.; Fryzuk, M. D. *J. Am. Chem. Soc.* **2006**, *128*, 12531. (i) Tanabe, Y.; Hanasaka, F.; Fujita, K.; Yamaguchi, R. *Organometallics* **2007**, *26*, 4618.

(17) (a) Hitchcock, P. B.; Lappert, M. F.; Pye, P. L. *J. Chem. Soc., Chem. Commun.* **1977**, 196. (b) Hitchcock, P. B.; Lappert, M. F.; Pye, P. L.; Thomas, S. *J. Chem. Soc., Dalton Trans.* **1979**, 1929. (c) Hitchcock, P. B.; Lappert, M. F.; Terreros, P. *J. Organomet. Chem.* **1982**, *239*, C26. (d) Huang, J.; Stevens, E. D.; Nolan, S. P. *Organometallics* **2000**, *19*, 1194. (e) Danopoulos, A. A.; Winston, S.; Hursthouse, M. B. *J. Chem. Soc., Dalton Trans.* **2002**, 3090. (f) Chilvers, M. J.; Jazzar, R. F. R.; Mahon, M. F.; Whittlesey, M. K. *Adv. Synth. Catal.* **2003**, *345*, 1111. (g) Giunta, D.; Hölscher, M.; Lehmann, C. W.; Mynott, R.; Wirtz, C.; Leitner, W. *Adv. Synth. Catal.* **2003**, *345*, 1139. (h) Abdur-Rashid, K.; Fedorkiw, T.; Lough, A. J.; Morris, R. H. *Organometallics* **2004**, *23*, 86. (i) Corberán, R.; Sanaú, M.; Peris, E. *J. Am. Chem. Soc.* **2006**, *128*, 3974. (j) Hong, S. H.; Chlenov, A.; Day, M. W.; Grubbs, R. H. *Angew. Chem., Int. Ed.* **2007**, *46*, 5148.

(18) An example of cyclometalation involving an alkenyl C−H bond: Cariou, R.; Fischmeister, C.; Toupet, L.; Dixneuf, P. H. *Organometallics* **2006**, *25*, 2126.

(19) Jazzar, R. F. R.; Macgregor, S. A.; Mahon, M. F.; Richards, S. P.; Whittlesey, M. K. *J. Am. Chem. Soc.* **2002**, *124*, 4944.

(20) (a) Edwards, M. G.; Jazzar, R. F. R.; Paine, B. M.; Shermer, D. J.; Whittlesey, M. K.; Williams, J. M. J.; Edney, D. D. *Chem. Commun.* **2004**, 90. (b) Burling, S.; Whittlesey, M. K.; Williams, J. M. J. *Adv. Synth. Catal.* **2005**, *347*, 591. (c) Burling, S.; Paine, B. M.; Nama, D.; Brown, V. S.; Mahon, M. F.; Prior, T. J.; Pregosin, P. S.; Whittlesey, M. K.; Williams, J. M. J. *J. Am. Chem. Soc.* **2007**, *129*, 1987.

(21) Diggle, R. A.; Macgregor, S. A.; Whittlesey, M. K. *Organometallics* **2004**, *23*, 1857.

example in which an NHC ligand is unstable with respect to displacement by a phosphine.

Computational Details

All calculations were run with Gaussian 03[22] and considered both small and full model systems with the aim of assessing both the electronic and steric effects of the NHC ligands. In the small models all phosphines were simplified to PH_3, while the nature of the NHC ligands depended on their role: the spectator IMes were represented by a simple imidazol-2-ylidene (IH) model, while a reacting IMes had one mesityl group replaced by H and the other simplified to an *o*-tolyl group (I*o*-tol). The parent six-coordinate complexes are therefore $Ru(PH_3)_3(CO)(H)_2$ (**6′**), Ru(I*o*-tol)$(PH_3)_2$-$(CO)(H)_2$ (**1′**$_{mono}$), and Ru(I*o*-tol)(IH)$(PH_3)(CO)(H)_2$ (**1′**$_{bis}$, the prime will be used to denote a small model species throughout). DFT calculations employing the BP86 functional were used with Ru and P centers described with the Stuttgart RECPs and associated basis sets[23] and an additional set of d-orbital polarization functions on P ($\zeta = 0.387$).[24] 6-31G** basis sets were used for all other atoms.[25] All stationary points were fully characterized via analytical frequency calculations as either minima (all positive eigenvalues) or transition states (one imaginary eigenvalue), and IRC calculations were used to confirm the minima linked by each transition state. Energies include a correction for zero-point energies.

Optimizations of the full systems were run with hybrid calculations within the ONIOM methodology implemented in Gaussian 03. In each case a reactive core was defined that corresponded to the small model systems described above, for which the same BP86 functional and ECP/basis set combinations were employed. The ONIOM approach also requires computation of the full molecule, and for this we have employed the Hartree−Fock level of theory with lanl2dz pseudopotentials and basis sets for Ru and P[26] (retaining d-orbital polarization on P) and 6-31G basis sets for all other atoms. Crystallographically characterized structures provided initial geometries for the optimization of **1**$_{mono}$,[27] **6**,[28] **3**$_{mono}$, and **5**.[19] No experimental structural data are available for **1**$_{bis}$, and in this case an initial geometry was obtained by adapting the structure of **1**$_{mono}$ by manually replacing the axial PPh_3 ligand with IMes. A conformational search using the "scan" facility of the Tinker program[29] was also used to ensure no low-energy structures were overlooked. Other stationary points were obtained via the reaction profiles discussed in the text. The nature of all stationary points was confirmed via analytical frequency calculations. Transition states were further characterized by displacing the geometry to mimic the unique imaginary frequency and then allowing these structures to relax to the adjacent local minima. The energies of all stationary points generated with the hybrid BP86/HF calculations were then recalculated with the BP86 functional, with Stuttgart RECPs and basis sets on Ru and P, d-orbital polarization functions on P, and 6-31G** basis sets on all other atoms. The zero-point energy corrections derived from the BP86/HF calculations were then applied to the BP86 SCF energies, and these BP86//BP86/HF values are quoted in the text. Free energies were obtained by applying the $T\Delta S$ corrections (25 °C) from the BP86/HF frequency calculations. Calculations on the full model systems incorporating general solvation via the polarized continuum model (PCM) approach[30] (benzene, $\epsilon = 2.247$) showed such medium effects to slightly reduce all the ligand dissociation processes, by ca. 2.5 kcal/mol for PPh_3 dissociation and by ca. 3.7 kcal/mol for IMes loss. Most importantly, however, the trends in ligand dissociation energies upon PPh_3/IMes substitution are unaffected. The PCM correction was found to be minimal (<1 kcal/mol) on the energetics of H_2 loss and all the bond activation processes (see Supporting Information for full details).

Results and Discussion

Summary of Experimental Ligand Exchange Processes. Previously we reported that PPh_3/IMes substitution in $Ru(PPh_3)_3(CO)(H)_2$ (**6**) to form Ru(IMes)$(PPh_3)_2(CO)(H)_2$ (**1**$_{mono}$) requires prolonged heating at 80 °C in benzene.[19] Subsequent studies have confirmed that no substitution occurs at 60 °C, even after extended periods. In contrast, PPh_3/IMes substitution in **1**$_{mono}$ occurs rapidly at room temperature to give $Ru(IMes)_2(PPh_3)(CO)(H)_2$ (**1**$_{bis}$), although after several hours an equilibrium is established in which **1**$_{mono}$ is again dominant. Thus **1**$_{mono}$ plus free IMes is more stable than **1**$_{bis}$ plus free PPh_3. This last observation accounts for the fact that the isolation of pure samples of **1**$_{bis}$ has proved elusive.[31]

Computed Ligand Exchange Processes. We have computed phosphine and NHC dissociation energies in **6**, **1**$_{mono}$, and **1**$_{bis}$, as well as their small model analogues. The computed geometries of **1**$_{mono}$ and **1**$_{bis}$ are shown in Figure 1. For **1**$_{mono}$ reasonable agreement with the experimental data is seen for distances and angles involving the heavy atoms, although the Ru−P bonds are somewhat overestimated by ca. 0.1 Å. A similar effect is also seen in the computed structures of **5**, **6**, and **3**$_{mono}$ where comparison with experiment is also available (see Supporting Information). This overestimation does not appear to be energetically significant, however, as recomputing the structure of **1**$_{mono}$ with the Ru−P distances fixed at their experimental values yields a structure that is only 1.5 kcal/mol higher in energy. It appears that the Ru−PPh_3 bonds in these species are associated with very soft potentials, and indeed this type of behavior has been noted previously in related Rh systems.[32]

The computed structures of **1**$_{mono}$ and **1**$_{bis}$ do show certain similarities, with longer Ru−H bonds being computed *trans* to CO while the "upper" IMes ligand (as shown in Figure 1) lies approximately parallel to the Ru−CO group. However some important differences point to greater steric encumbrance in **1**$_{bis}$, in particular a lengthening of the Ru−P1 and Ru−C2 distances by about 0.04 Å and a narrowing of the C1−Ru−P1 angle, from 102.9° in **1**$_{mono}$ to 85.6° in **1**$_{bis}$. This reduced angle arises from the presence of four mesityl groups in **1**$_{bis}$, which severely restrict the space available to the remaining PPh_3 ligand. For the small models, where steric hindrance is minimal, the C1−Ru−P1 angle is consistently around 102°. One useful measure of steric encumbrance in the bis-IMes systems is the extent to which the IMes ligands are forced to lie parallel to each other, as given by the average N−C2−C3−N torsion angle. In **1**$_{bis}$ this is only 15°.

(22) Frisch, M. J.; et al. *Gaussian 03, Revision C.02*; Gaussian, Inc.: Wallingford, CT, 2004.
(23) Andrae, D.; Häusserman, U.; Dolg, M.; Stoll, H.; Preuss, H. *Theor. Chim. Acta* **1990**, *77*, 123.
(24) Höllwarth, A.; Böhme, M.; Dapprich, S.; Ehlers, A. W.; Gobbi, A.; Jonas, V.; Köhler, K. F.; Stegmann, R.; Veldkamp, A.; Frenking, G. *Chem. Phys. Lett.* **1993**, *208*, 237.
(25) (a) Hehre, W. J.; Ditchfield, R.; Pople, J. A. *J. Chem. Phys.* **1972**, *56*, 2257. (b) Hariharan, P. C.; Pople, J. A. *Theor. Chim. Acta* **1973**, *28*, 213.
(26) Hay, P. J.; Wadt, W. R. *J. Chem. Phys.* **1985**, *82*, 299.
(27) Jazzar, R. F. R. Ph.D. Thesis, University of Bath, 2003.
(28) Junk, P. C.; Steed, J. W. *J. Organomet. Chem.* **1999**, *587*, 191.
(29) Pappu, R. V.; Hart, R. K.; Ponder, J. W. *J. Phys. Chem. B* **1998**, *102*, 9725.
(30) Cancèst, M. T. B.; Mennucci, B.; Tomasi, J. *J. Chem. Phys.* **1997**, *107*, 3032.
(31) Chatwin, S. L.; Davidson, M. G.; Doherty, C.; Donald, S. M.; Jazzar, R. F. R.; Macgregor, S. A.; McIntyre, G. J.; Mahon, M. F.; Whittlesey, M. K. *Organometallics* **2006**, *25*, 99.
(32) Macgregor, S. A.; Wondimagegn, T. *Organometallics* **2007**, *26*, 3651.

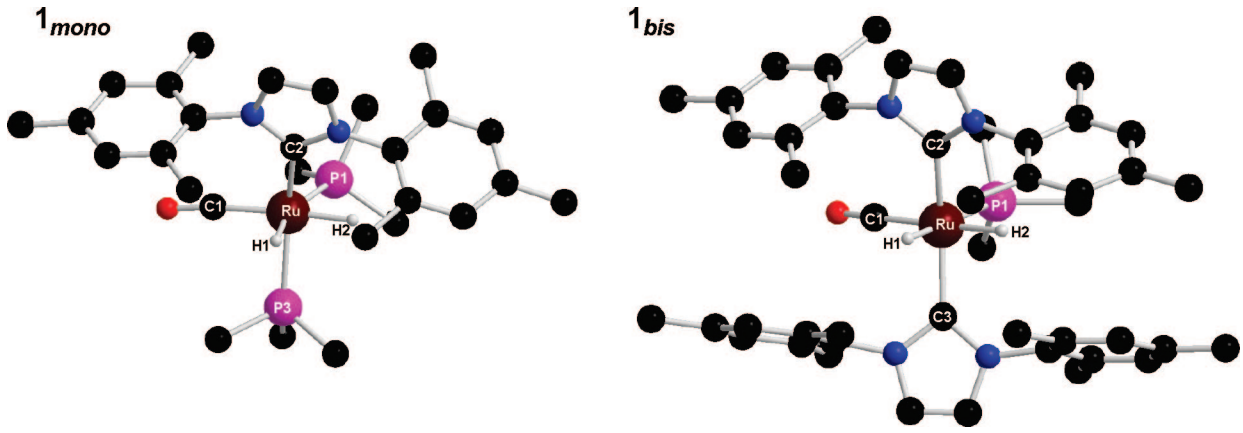

Figure 1. Computed structures of $\mathbf{1}_{mono}$ and $\mathbf{1}_{bis}$. For clarity PPh_3 phenyl groups are truncated at the *ipso* carbon and IMes H atoms are omitted. Key distances (Å) and angles (deg) with equivalent experimental data for $\mathbf{1}_{mono}$ in italics,[27] $\mathbf{1}_{mono}$: Ru−P1 = 2.459/*2.3628(4)*; Ru−P3 = 2.390/*2.2985(5)*; Ru−C1 = 1.910/*1.9145(17)*; Ru−C2 = 2.085/*2.0956(17)* Ru−H1 = 1.610/*1.57(2)*; Ru−H2 = 1.653/*1.55(2)*; C1−Ru−P1 = 102.9/*100.65(5)*; C2−Ru−P3 = 151.3/*146.33(5)*; P1−Ru−P3 = 100.6/*102.115(16)*. $\mathbf{1}_{bis}$: Ru−P1 = 2.498; Ru−C1 = 1.910; Ru−C2 =2.125; Ru−C3 = 2.131; Ru−H1 = 1.612; Ru−H2 = 1.658; C1−Ru−P1 = 85.6; C2−Ru−C3 = 153.0; C3−Ru−P1 = 101.7; N−C2−C3−N (av) = 15.

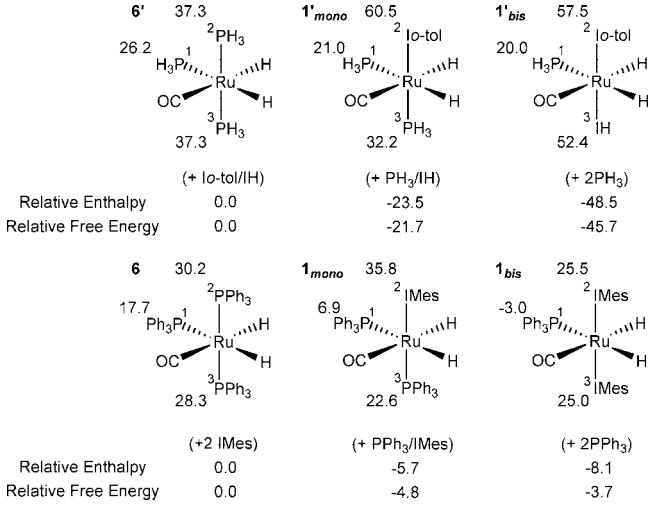

Figure 2. Computed phosphine and NHC ligand dissociation energies (kcal/mol) in **6**, $\mathbf{1}_{mono}$, and $\mathbf{1}_{bis}$ and their small model analogues. Computed relative enthalpies and free energies associated with the equilibria linking these species are also indicated.

The computed phosphine and NHC ligand dissociation energies are summarised in Figure 2. For the small models dissociation of the Ru−$^1PH_3$ bond is always the easiest process, and this reflects the high *trans* influence of the hydride ligand. $^1PH_3$ loss is 5 kcal/mol easier in $\mathbf{1'}_{mono}$ than in **6′**; however this does not reflect a weakening of the Ru−P bond as such, but rather a stabilization of the Ru(I*o*-tol)(PH_3)(CO)$(H)_2$ species that is formed. The square-pyramidal structure of this species in which hydride is axial (T_H) allows for the presence of a strong agostic interaction with one C−H bond of the *o*-Me group at the vacant coordination site. On going from $\mathbf{1'}_{mono}$ to $\mathbf{1'}_{bis}$ the Ru−$^1PH_3$ dissociation remains at around 20 kcal/mol, as no additional agostic stabilization is possible in T_H Ru(I*o*-tol)-(IH)(CO)$(H)_2$. The small models confirm the expected higher *trans* influence of simple NHCs over PH_3, with the Ru−$^3PH_3$ bond being weakened by 5 kcal/mol on going from **6′** to $\mathbf{1'}_{mono}$ and the Ru−^{2}I*o*-tol bond weakening by 3 kcal/mol between $\mathbf{1'}_{mono}$ and $\mathbf{1'}_{bis}$. In the 2 and 3 "axial" positions the Ru−NHC bonds are significantly stronger than the Ru−P bonds, and this is reflected in the very favorable energetics computed for PH_3/NHC substitution, which in each case is accompanied by a stabilization of approximately 24 kcal/mol.

Inclusion of the full steric bulk of the IMes and PPh_3 ligands results in a significant reduction in all the ligand dissociation energies. Loss of phosphine *trans* to hydride is again the most facile process, and for **6** this is 8.5 kcal/mol easier than for **6′**. Each PPh_3/IMes substitution further labilizes the Ru−$^1PPh_3$ bond by about 10 kcal/mol; however, for the full systems no significant agostic stabilization is apparent in the five-coordinate T_H species formed. Instead the easier $^1PPh_3$ loss reflects an increasing degree of steric encumbrance in the six-coordinate species upon each PPh_3/IMes substitution. Figure 3 displays the computed structure of T_H Ru$(IMes)_2(CO)(H)_2$ ($\mathbf{7}_{bis}$) and shows how the IMes ligands rotate to make use of the space vacated by the PPh_3 ligand. This relief of steric strain is reflected in an increase in the average N−C2−C3−N torsion to 51°. The $^1PPh_3$ ligand in $\mathbf{1}_{bis}$ appears to be particularly affected by being positioned between two large, relatively inflexible IMes ligands, and $\mathbf{1}_{bis}$ is actually computed to be unstable with respect to T_H Ru$(IMes)_2(CO)(H)_2$ and free PPh_3.[33] In the 2 and 3 "axial" positions the same trends computed above for the small models are again seen, with the higher *trans* influence of IMes labilizing the Ru−$^3PPh_3$ bond in $\mathbf{1}_{mono}$ and the Ru−^{2}IMes bond in $\mathbf{1}_{bis}$. The Ru−NHC dissociation energies are significantly affected by the increased steric bulk, and in $\mathbf{1}_{bis}$ the values for the NHC ligands are less than half those computed for $\mathbf{1'}_{bis}$. In contrast the Ru−$^{2/3}PPh_3$ dissociation energies are only about 10 kcal/mol lower than in the small systems. As a result, PPh_3/IMes substitution is far less favorable in the full model systems and the computed enthalpies for these processes are only slightly exothermic. Indeed, the computed free energies suggest that $\mathbf{1}_{mono}$ plus free IMes and PPh_3 is the most stable combination, mirroring what is seen experimentally.

Formation of Reactive Ru(0) Intermediates. In order to induce C−C (or C−H) bond activation in $\mathbf{1}_{mono}$ and $\mathbf{1}_{bis}$, removal

(33) Although the binding energy of $^1PPh_3$ in $\mathbf{1_{bis}}$ is negative, this species does correspond to a local minimum, and a computed profile based on the Ru−^{1}P distance provides an estimated activation energy for PPh_3 loss of around 5 kcal/mol. The absolute values of the free energies should be treated with caution, as effects such as specific solvation are not taken into account in our calculations. More reliable are the computed trends, and these clearly indicate an increasing ease of phosphine dissociation along the series **6** to $\mathbf{1}_{mono}$ to $\mathbf{1}_{bis}$. This is consistent with the difficulty of isolating pure samples of $\mathbf{1}_{bis}$.[31]

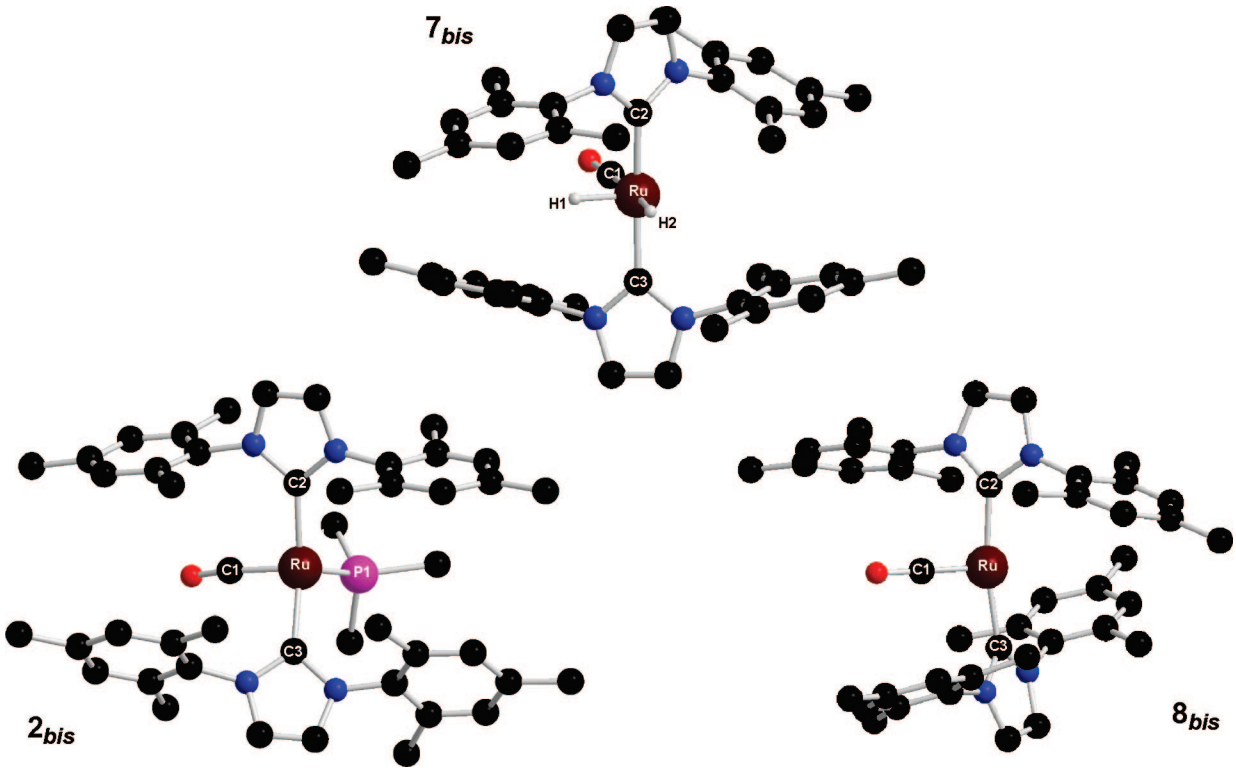

Figure 3. Computed structures of the unsaturated intermediates derived from $\mathbf{1}_{bis}$ via PPh_3 and H_2 loss. For clarity PPh_3 phenyl groups are truncated at the *ipso* carbon and IMes H atoms are omitted. Key distances (Å) and angles (deg) $\mathbf{2}_{bis}$: Ru−P1 = 2.400; Ru−C1 = 1.809; Ru−C2 = 2.108; Ru−C3 = 2.130; C1−Ru−P1 = 108.1; C2−Ru−C3 = 150.9; N−C2−C3−N (av) = 22. $\mathbf{7}_{bis}$: Ru−C1 = 1.881; Ru−C2 = 2.071; Ru−C3 = 2.066; Ru−H1 = 1.541; Ru−H2 = 1.696; C2−Ru−C3 = 168.6; N−C2−C3−N (av) = 51. $\mathbf{8}_{bis}$: Ru−C1 = 1.760; Ru−C2 = 2.065; Ru−C3 = 2.040; C2−Ru−C3 = 169.6; N−C2−C3−N (av) = 80.

of H_2 is required, and under the reaction conditions this is assumed to take place via thermal reductive elimination to produce reactive Ru(0) intermediates.[34] This may occur either directly at the six-coordinate species to give four-coordinate **2** or at five-coordinate T_H **7** to give the three-coordinate species **8**. These latter 14e species can also be formed via PPh_3 loss from **2**. The energetics of all these various processes are summarized in Figure 4. In addition, following a suggestion of a referee, we also considered the possibility of specific solvation of these unsaturated species by a benzene molecule. For **2** and **7** all attempts to locate such an adduct led to benzene dissociation. For $\mathbf{8}_{mono/bis}$, however, local minima featuring a weak C−H agostic interaction with benzene were found, although these were computed to be between 2 and 4 kcal/mol less stable than isolated $\mathbf{8}_{mono/bis}$ plus free benzene. No η^2-complexes could be located. We therefore conclude that such specific solvation does not play a significant role in stabilizing any of the unsaturated species **2**, **7**, or **8**. This is consistent with a strong degree of steric protection that is afforded to the metal by the presence of bulky IMes and PPh_3 ligands.

In general, the energy required to remove H_2 from either **1** or **7** shows relatively little variation, although this process is certainly not promoted by PPh_3/IMes substitution, it being hardest in $\mathbf{1}_{bis}$ (ΔH = +28.4 kcal/mol). The major reason for this is again steric in origin. Normally $Ru(CO)L_3$ species adopt

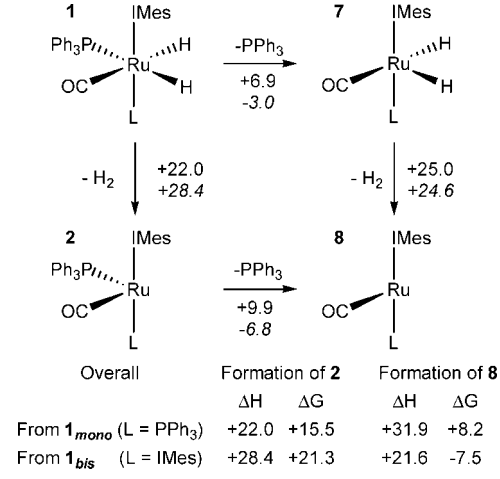

Figure 4. Computed energies (kcal/mol) for PPh_3 and H_2 loss steps derived from $\mathbf{1}_{mono}$ (L = PPh_3) and $\mathbf{1}_{bis}$ (L = IMes, in italics). The total enthalpies and free energies of formation for intermediates **2** and **8** are also indicated.

a distorted butterfly geometry in which the *trans*-OC−Ru−L angle is about 140°, and this geometry was indeed located with the small models $\mathbf{2'}_{mono}$ and $\mathbf{2'}_{bis}$.[21,35] However, for the full systems, the OC−Ru−P1 angles are somewhat smaller, namely, 121.5° in $\mathbf{2}_{mono}$ and only 108.1° in $\mathbf{2}_{bis}$ (see Figure 3). One effect of the bulky ligands is therefore to prevent the geometry of these unsaturated species relaxing to their ideal form. As this effect is particularly marked for $\mathbf{2}_{bis}$, this results in the increased

(34) A number of alternative pathways were tested with the smaller **1′** models. These included C−C bond activation at five-coordinate **7′** to give Ru(IV) intermediates or, after C−H activation to form an intermediate such as **10**, C−C activation via α-migration of an aryl substituent to give a Ru=CH_2 species. However, these processes proved to have far higher activation energies than simple oxidative addition at **8′** or **2′**, and so were discarded on this basis.

(35) Ogasawara, M.; Macgregor, S. A.; Streib, W. E.; Folting, K.; Eisenstein, O.; Caulton, K. G. *J. Am. Chem. Soc.* **1996**, *118*, 10189.

Table 1. Computed Energetics (kcal/mol) for C−C and C−H Activation in $2_{mono}/2_{bis}$ and $8_{mono}/8_{bis}$

	$\Delta H^{\ddagger}/\Delta G^{\ddagger}_{C-C}$	$\Delta H/\Delta G_{C-C}$	$\Delta H^{\ddagger}/\Delta G^{\ddagger}_{C-H}$	$\Delta H/\Delta G_{C-H}$
$\mathbf{2}_{mono}$	+26.2/+28.2	−1.6/−1.0	+12.1/+13.1	−11.2/−10.4
$\mathbf{2}_{bis}$	+32.0/+32.4	−1.4/−1.0	+10.0/+10.2	−12.8/−11.9
$\mathbf{8}_{mono}$	+24.5/+23.5	−5.4/−5.6	+3.6/+3.7	−16.4/−16.5
$\mathbf{8}_{bis}$	+23.5/+26.9	−6.6/−4.4	+0.5/+3.4	−15.4/−12.7

energy associated with H_2 loss. The significant steric encumbrance retained in $\mathbf{2}_{bis}$ is reflected in the average N−C2−C3−N torsion of 22°.[36] As was seen in the six-coordinate species, phosphine dissociation from the four-coordinate systems is strongly promoted by the presence of a second IMes ligand and is actually exothermic relative to $\mathbf{2}_{bis}$. This is again due to the relief of steric crowding in the bis-IMes systems that occurs upon PPh_3 loss, and the three-coordinate species formed, $\mathbf{8}_{bis}$, is able to adopt a very open structure in which the IMes ligands are almost perpendicular (N−C2−C3−N (av) = 80°, see Figure 3). Despite the fact that $\mathbf{8}_{bis}$ is a highly unsaturated 14e species, there is no evidence of any significant interaction between the Ru center and any of the mesityl *o*-Me groups, with the nearest contact being over 3.2 Å.

Overall, the major effect of PPh_3/IMes substitution in **6**, $\mathbf{1}_{mono}$, and $\mathbf{1}_{bis}$ is to strongly facilitate PPh_3 dissociation *trans* to hydride, particularly in the bis-IMes systems. The formation of the three-coordinate intermediate $\mathbf{8}_{bis}$ from $\mathbf{1}_{bis}$ is particularly favored and requires only 21.6 kcal/mol. In comparison the formation of $\mathbf{8}_{mono}$ from $\mathbf{1}_{mono}$ requires 31.9 kcal/mol. The enthalpy of formation of $\mathbf{8}_{bis}$ is only marginally less favorable than those of the alternative four-coordinate species $\mathbf{2}_{mono}$ and $\mathbf{2}_{bis}$; however, the formation of the three-coordinate species will also be driven by the entropy associated with the release of both H_2 and PPh_3. This strongly favors the formation of $\mathbf{8}_{bis}$, and the free energy of formation of this species relative to $\mathbf{1}_{bis}$ is −7.5 kcal/mol, over 15 kcal/mol more favorable than any of the alternative reactive intermediates.

Intramolecular Bond Activation. We have computed the energetics of intramolecular C−C activation and the potentially competing intramolecular C−H activation for the four-coordinate species $\mathbf{2}_{mono}$ and $\mathbf{2}_{bis}$ as well as the three-coordinate species $\mathbf{8}_{mono}$ and $\mathbf{8}_{bis}$.[37] The results are summarized in Table 1, while Figure 5 illustrates the reactivity of the most accessible intermediate, $\mathbf{8}_{bis}$. The behavior of $\mathbf{8}_{bis}$ is representative of all the species considered, and so full details of the species involved in these other reaction profiles are reserved for the Supporting Information. Given the importance of entropic effects in determining the formation of the reactive intermediates, we shall focus on the computed free energies in the following, although the computed enthalpies will also be indicated. For $\mathbf{8}_{bis}$ C−C activation occurs with a free energy barrier of 26.9 kcal/mol via $\mathbf{TS(8–9)}_{bis}$. This transition state exhibits a very late structure, with the relevant C−C bond lengthening to 1.87 Å, while the Ru−aryl bond (2.16 Å) is effectively already fully formed at this stage. In contrast, the free energy barrier for C−H activation is only 3.4 kcal/mol, although the transition state, $\mathbf{TS(8–10)}_{bis}$, still displays significant C−H bond lengthening. The C−H and C−C bond activation products are five-coordinate square-pyramidal species with either an apical hydride ($\mathbf{10}_{bis}$, G = −20.2 kcal/mol) or methyl ($\mathbf{9}_{bis}$, G = −11.9 kcal/mol), and it is noticeable that the structure of the latter features a long Ru−C distance to the spectator IMes ligand. This presumably arises from the steric crowding arising from the rigid cyclometalated aryl moiety, which necessarily impinges on the space available to the second IMes ligand.

The data in Table 1 show that the three other unsaturated species exhibit the same general behavior as $\mathbf{8}_{bis}$. Thus in every case C−H activation is favored both kinetically and thermodynamically over C−C activation as an individual reaction step. The higher computed barriers to C−C activation are expected, as this process is known to require significant distortion of the C−C bond in order to permit sufficient interaction with the metal center.[38] In addition, the greater exothermicity of C−H over C−C activation reflects the fact that late TM−hydride bonds are significantly stronger than equivalent TM−alkyl bonds, although this difference will be offset to some extent here by the greater strength of the Ru−aryl bond formed upon C−C activation compared to the Ru−benzyl bond resulting from C−H activation.[39] Within the data in Table 1 there are some variations in behavior. For example, intramolecular bond activation is more favorable at the three-coordinate species, which feature lower activation barriers and higher exothermicities compared to the related four-coordinate species. This may be due to the ability of the T-shaped ML_3 molecules to undergo reaction without requiring any substantial reorganization of the metal coordination geometry. In contrast, in the four-coordinate systems the OC−Ru−P1 angle must narrow during oxidative addition, and this is disfavored, especially in the presence of bulky ligands. Thus for C−C bond activation the introduction of the second IMes ligand in $\mathbf{2}_{bis}$, far from promoting C−C activation, actually increases the activation barrier to 32 kcal/mol. In contrast in three-coordinate $\mathbf{8}_{mono}$ and $\mathbf{8}_{bis}$ the C−C activation barriers are relatively unaffected by PPh_3/IMes substitution.

In terms of accounting for the experimental observation of C−C bond activation in $\mathbf{1}_{bis}$ the data in Table 1 indicate that once any of the three- or four-coordinate intermediates are formed, they would preferentially undergo rapid C−H activation. However, the barrier for the reverse process is relatively modest (only 16.1 kcal/mol in the case of $\mathbf{10}_{bis}$), and so in the absence of any reaction that would trap the C−H activation product this process may be reversible. At sufficiently high temperatures the much higher barrier to C−C activation may then be surmounted. Confirmation that this C−C activation event has occurred still requires a C−C activation product to be trapped irreversibly, and experimentally this occurs through the further reaction of species such as $\mathbf{9}_{bis}$ with H_2 and PPh_3 to give **5**, the ultimate observed product of C−C activation. This further reactivity will be considered below.

Combining the data on H_2 and PPh_3 loss with those on C−C bond activation allows the overall reaction profiles for C−C activation in $\mathbf{1}_{mono}$ and $\mathbf{1}_{bis}$ to be constructed (see Figure 6), and we shall again focus on the free energies because of the importance of ligand dissociation in distinguishing the accessibility of the various unsaturated species involved. Indeed given that there is relatively little variation in the barriers for the C−C activation step, it is the ease of H_2 loss and in particular PPh_3 dissociation that determines which will be the most favored overall pathway. The very easy formation of $\mathbf{8}_{bis}$ therefore leads to the lowest overall pathway for C−C activation, which proceeds via $\mathbf{TS(8–9)}_{bis}$ with a free energy of activation of only

(36) Other geometries for the structure of $\mathbf{2}_{bis}$ were also assessed, and an alternative minimum with a square-planar geometry was located. However, this proved to be 3 kcal/mol higher in energy than the structure reported in the text.

(37) C−C and C−H activation were also studied with the small model systems, and very similar behavior was computed in all cases. For the small models C−C activation is slightly more accessible ($\Delta E^{\ddagger} \approx 21$ kcal/mol), and this process is more exothermic ($\Delta E \approx -11$ kcal/mol).

(38) Low, J. J.; Goddard, W. A., III. *J. Am. Chem. Soc.* **1986**, *108*, 6115.
(39) Simões, J. A. M.; Beauchamp, J. L. *Chem. Rev.* **1990**, *90*, 629.

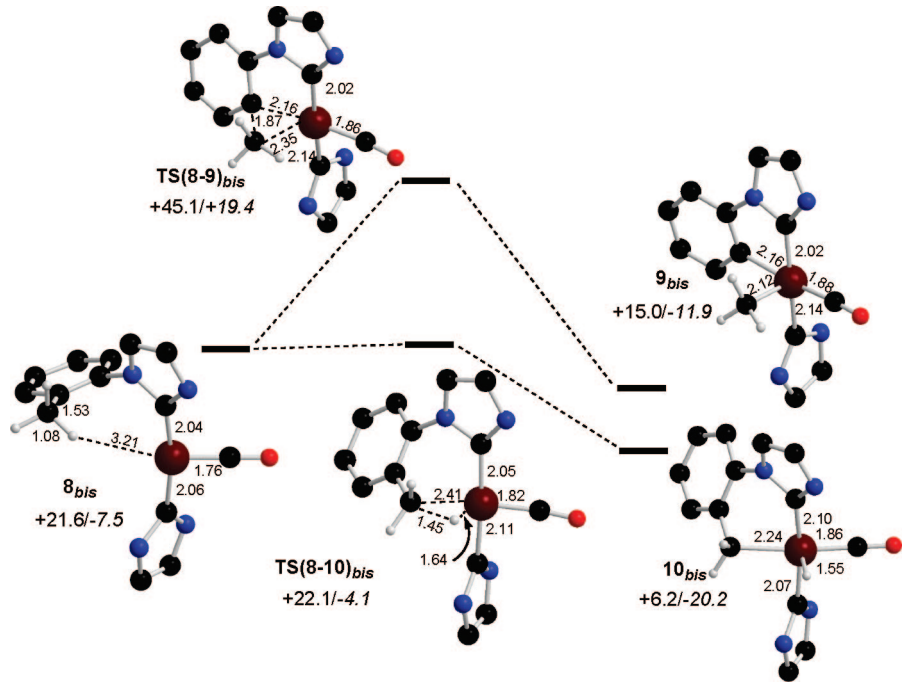

Figure 5. Computed reaction profiles (kcal/mol) for C−C and C−H activation in $\mathbf{8}_{bis}$ with selected distances in Å. Energies are relative to $\mathbf{1}_{bis}$ at 0.0 kcal/mol, and free energies are given in italics. For the IMes ligands only the *o*-Me group involved in activation is shown, while all other substituents and IMes backbone H atoms are omitted for clarity.

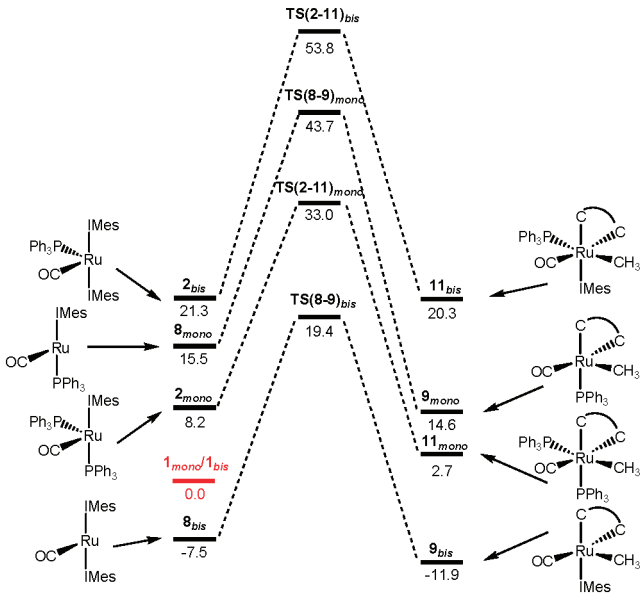

Figure 6. Computed free energy reaction profiles (kcal/mol) for C−C activation in $\mathbf{1}_{mono}$ and $\mathbf{1}_{bis}$. Data are quoted relative to $\mathbf{1}_{mono}$ and $\mathbf{1}_{bis}$ set to zero (indicated in red).

19.4 kcal/mol. This is almost 14 kcal/mol below **TS(2–11)**$_{mono}$ (G = +33.0 kcal/mol), while to even higher energy lie **TS(8–9)**$_{mono}$ (G = +43.7 kcal/mol) and **TS(2–11)**$_{bis}$ (G = +53.8 kcal/mol). These results now account for the need to have two IMes ligands present before C−C activation is observed in $\mathbf{1}_{bis}$, and this can be traced to the promoting effect of the second IMes ligand on PPh_3 dissociation, which, along with the favorable entropic character of this process, renders highly reactive intermediates such as $\mathbf{8}_{bis}$ accessible.

The relative accessibility of C−C activation in $\mathbf{8}_{bis}$ (as well as $\mathbf{2}_{mono}$ and $\mathbf{8}_{mono}$) is also worthy of comment.[40] In many cases C−C bond activation requires a clear thermodynamic driving force to promote the reaction, for example relief of ring strain, or stabilization of the product through a gain in aromaticity.[41] Cyclometalation reactions similar to those considered here have also been observed in other ligand systems,[42,43] and Milstein and co-workers have reported particularly detailed studies of C(sp^2)−C(sp^3) bond activation in phosphine-based pincer ligands, which in many cases can occur at or even below room temperature.[44] In these systems the architecture of the pincer ligand promotes reaction by placing the C−C bond in close proximity to the metal center. In certain cases C−C activation is actually kinetically favored over C−H activation,[45] and an activation enthalpy of 15.0 (±0.4) kcal/mol has been determined experimentally for a PCN/Rh(I) ligand system.[46] Generally, C−C bond activation is thermodynamically favored in these systems, and this has been attributed to the more stable five-

(40) (a) For reviews, see: Rybtchinski, B.; Milstein, D. *Angew. Chem., Int Ed.* **1999**, *38*, 870. (b) Murakami, M.; Ito, Y. In *Topics in Organometallic Chemistry*; Murai, S., Ed.; Springer: Berlin, 1999; Vol. 3, p 97. (c) Jun, C.-H. *Chem. Soc. Rev.* **2004**, 610.

(41) (a) Bishop, K. C., III. *Chem. Rev.* **1976**, *76*, 461. (b) Crabtree, R. H. *Chem. Rev.* **1985**, *85*, 245. (c) Chaudret, B. *Bull. Soc. Chim. Fr.* **1995**, *132*, 268. (d) DiMauro, P. T.; Wolczanski, P. T. *Polyhedron* **1995**, *14*, 195. (e) Perthuisot, C.; Edelbach, B. L.; Zubris, D. L.; Simhai, N.; Iverson, C. N.; Müller, C.; Satoh, T.; Jones, W. D. *J. Mol. Catal. A* **2002**, *189*, 157.

(42) Examples with 8-quinolinyl alkyl ketones: Suggs, J. W.; Jun, C.-H. *J. Am. Chem. Soc.* **1986**, *108*, 4679, and references therein.

(43) For examples based on NCN pincers, see: Steenwinkel, P.; Gossage, R. A.; van Koten, G. *Chem.−Eur. J.* **1998**, *4*, 759.

(44) (a) van Koten, G.; Albrecht, M. *Angew. Chem. Int. Ed.* **2001**, *40*, 3750. (b) van der Boom, M. E.; Milstein, D. *Chem. Rev* **2003**, *103*, 1759 and references therein.

(45) (a) Rybtchinski, B.; Vigalok, A.; Ben-David, Y.; Milstein, D. *J. Am. Chem. Soc.* **1996**, *118*, 12406. (b) Gandelman, M.; Vigalok, A.; Shimon, L. J. W.; Milstein, D. *Organometallics* **1997**, *16*, 3981. (c) Rybtchinski, B.; Milstein, D. *J. Am. Chem. Soc.* **1999**, *121*, 4528. (d) Salem, H.; Ben-David, Y.; Shimon, L. J. W.; Milstein, D. *Organometallics* **2006**, *25*, 2292.

(46) (d) Gandelman, M.; Vigalok, A.; Konstantinovski, L.; Milstein, D. *J. Am. Chem. Soc* **2000**, *122*, 9848. Computed barriers to C−C activation in PCP/Rh(I) systems are in the range 10–17 kcal/mol, depending on the phosphine substituent. See ref 47.

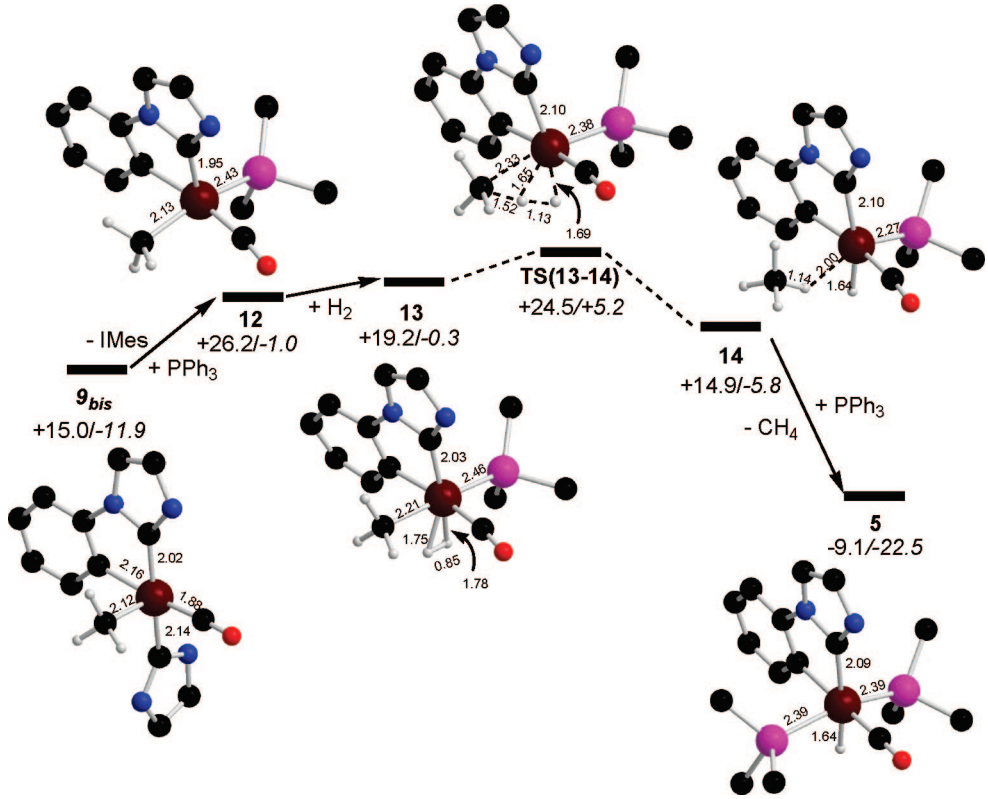

Figure 7. Computed reaction profile (kcal/mol, relative to $\mathbf{1}_{bis}$) for the formation of **5** from $\mathbf{9}_{bis}$. Free energies given in italics with selected distances in Å. Only the aryl group of the C−C activated IMes ligand is shown, with all other IMes substituents omitted for clarity. Similarly, PPh_3 ligands are truncated at the *ipso* carbon.

membered metallacycle formed in this process, as compared to a strained six-membered ring that results from C−H activation.[47]

In contrast, the reasons for accessible C(sp^2)−C(sp^3) activation in $\mathbf{8}_{bis}$ are not so clear. The structure of this species does not suggest any kinetic predisposition of the ligand to C−C bond cleavage, as the relevant carbon atoms are initially more than 4.0 Å away from the metal center. C−C activation in $\mathbf{8}_{bis}$ is exogenic, and the favorable thermodynamics of this process clearly reflects its intramolecular nature. Additional factors that may facilitate C−C activation are the formation of a strong Ru−C(aryl) bond and the fact that in the cyclometalated ligand the activated aryl group is coplanar with the imidazole ring and so may benefit from improved conjugation through the π-system. Overall, however, the ability of species such as $\mathbf{8}_{bis}$ to effect C−C activation may simply be due to their extremely high reactivity. Studies on related Ru(0) species such as $Ru(R_2PCH_2CH_2PR_2)_2$ (R = Me, Et, Ph) have shown remarkably high rate constants for H−H and C−H bond activation.[48] This behavior has been linked to the extremely electron-rich nature of such Ru(0) species compared to isoelectronic (but less electron-rich) Rh^+ analogues.[49]

Formation of 5. Once C−C activation has occurred at $\mathbf{8}_{bis}$, the subsequent reaction of the product, $\mathbf{9}_{bis}$, with H_2 and PPh_3 must take place in order to yield the final observed product, **5**. A number of pathways can be envisaged for this transformation, but we shall discuss only one possibility, shown in Figure 7. Addition of PPh_3 to $\mathbf{9}_{bis}$ produces $\mathbf{11}_{bis}$, from which IMes dissociation yields the five-coordinate intermediate, **12** (G = −1.0 kcal/mol). As in $\mathbf{1}_{bis}$, IMes/PPh_3 substitution again appears to be a relatively accessible process, and in this case this will be aided by the crowded nature of $\mathbf{9}_{bis}$, noted above, due to the presence of the rigid cyclometalated aryl moiety. **12** maintains a square-pyramidal geometry with a vacant site *trans* to the cyclometalated IMes ligand. Addition of H_2 therefore produces a dihydrogen complex, **13** (G = −0.3 kcal/mol), in which the η^2-H_2 ligand is *cis* to methyl. **13** is set up for a σ-bond metathesis step, which proceeds with a small free energy barrier of only 5.5 kcal/mol to produce a weakly bound CH_4 adduct, **14** (G = −5.8 kcal/mol). Displacement of CH_4 by PPh_3 then produces **5**. Importantly, none of the stationary points in Figure 7 is higher in free energy than the preceding C−C activation transition state, $\mathbf{TS(8\text{-}9)}_{bis}$, at +19.4 kcal/mol. This means that, once formed, $\mathbf{9}_{bis}$ will readily be trapped by reaction with H_2 and PPh_3 to give **5**.

Previously, we noted that C−H activation is more accessible than C−C activation at species such as $\mathbf{8}_{bis}$, although no cyclometalated species derived from C−H activation in the bis-IMes systems has been observed. It is worth noting that the reaction of $\mathbf{10}_{bis}$, the initial C−H activated product formed from $\mathbf{8}_{bis}$, with H_2 would simply lead to exchange at the Ru−H ligand position and so would not trap out the C−H activated product in the same way that loss of CH_4 from the reaction of $\mathbf{9}_{bis}$ with H_2 allows us to recognize that C−C activation has taken place. A facile H exchange process coupled with reversible C−H activation would suggest that H/D scrambling at the *o*-Me position of the IMes ligands would be observed if the reaction were carried out with appropriately labeled species. Experiments

(47) Sundermann, A.; Uzan, O.; Milstein, D.; Martin, J. M. L. *J. Am. Chem. Soc.* **2000**, *122*, 7095.

(48) (a) Hall, C.; Jones, W. D.; Mawby, R. J.; Osman, R.; Perutz, R. N.; Whittlesey, M. K. *J. Am. Chem. Soc.* **1992**, *114*, 7425. (b) Cronin, L.; Nicasio, M. C.; Perutz, R. N.; Peters, R. G.; Roddick, D. M.; Whittlesey, M. K. *J. Am. Chem. Soc.* **1995**, *117*, 10047.

(49) Macgregor, S. A.; Eisenstein, O.; Whittlesey, M. K. Perutz, R. N. *J. Chem. Soc., Dalton Trans.* **1998**, 291.

with $Ru(IMes)_2(PPh_3)(CO)(D)_2$ indicate that such scrambling does indeed occur.[50]

Conclusions

We have used DFT calculations to account for the observation of the unusual C−C bond activation reaction of $Ru(IMes)_2(PPh_3)(CO)(H)_2$, $\mathbf{1}_{bis}$. The calculations show that the formation of a bis-IMes species leads to a marked labilization of the remaining PPh_3 ligand, and this, coupled to H_2 loss, results in the formation of a highly reactive 14e intermediate $Ru(IMes)_2(CO)$, $\mathbf{8}_{bis}$. Although C−H activation is more accessible in $\mathbf{8}_{bis}$ than C−C activation, the former process is expected to be reversible, and so C−C activation becomes possible at elevated temperatures. The initial C−C activated product is then readily trapped by further reaction with H_2 and PPh_3. The presence of a second IMes ligand does not specifically promote the C−C bond activation step as such, but rather promotes the formation of a reactive intermediate that is then capable of inducing this process. Similarly, significant steric encumbrance in $\mathbf{1}_{bis}$ renders this species unstable with respect to displacement of an IMes ligand by PPh_3. The calculations also suggest that alternative intermediates such as $Ru(IMes)(PPh_3)(CO)$ ($\mathbf{8}_{mono}$) or $Ru(IMes)(PPh_3)_2(CO)$ ($\mathbf{2}_{mono}$) will also be highly reactive to intramolecular bond activation processes. Therefore, any process where such reactive Ru(0) intermediates are accessible may be susceptible to intramolecular bond activation reactions that could undermine the integrity of any N-aryl NHC that is present.

Acknowledgment. We thank the EPSRC, the University of Bath, and Heriot-Watt University for support.

Supporting Information Available: Tables of computed Cartesian coordinates and energies of all species. Full reference 22. This material is available free of charge via the Internet at http://pubs.acs.org.

OM700977F

(50) Burling, S.; Whittlesey, M. K., unpublished results.